CONSTRUCTION OF A THERMAL INERTIA MAPPING SYSTEM (TIMS) FOR HYDROLOGICAL ANALYSIS OF THE EARTH'S SURFACE USING SATELLITE AND GROUND MONITORING DATA

YOJIRO UTSUNOMIYA

Water and Soil Environment Div., National Institute
for Environmental Studies, Environment Agency,
16-2 Onogawa, Tsukuba, Ibaraki 305, Japan

Commission IV, Working Group 6

KEY WORDS: Remote sensing, Environment, Hydrology, soil, database, GIS

ABSTRACT:

In order to construct a prototype database system for heat balance analysis (Thermal Inertia Mapping System: TIMS) and hydrological evaluation in and around the Japan Islands, we constructed prototype water temperature and meteorological databases and a main processing system for thermal inertia mapping from aerometeorological and ground monitoring and NOAA satellite data. The components of the system were as follows: 1) Prototype database system for water temperature and meteorological monitoring in Japan. 2) Rectification system for NOAA AVHRR imagery. 3) Heat balance analysis, a) Shortwave radiation: i) albedo estimation, ii) albedo correction (absolute albedo), iii) albedo normalization and surface relative moisture, b) Long wave radiation: i) calculation of downward and upward radiation, ii) effective radiation, c) net radiation. 4) Calculation of diffusion coefficient. 5) Calculation of thermal inertia.

1. INTRODUCTION

The author has developed a thermal inertia model and applied it to airborne MSS and ground monitoring micro-meteorological data. We applied this procedure to NOAA AVHRR data and obtained satisfactory results in areas from the semi-arid to arid climatic regions of northeastern China. As several problems with the estimation of parameter such as absolute albedo, relative soil surface wetness, short and long wave radiation, net radiation, diffusion coefficient and cloud screening in these broad areas (for about 512x512 km) remained for this procedure, a further study was conducted, and successful results were recently obtained by construction of a thermal inertia mapping prototype system (TIMS). To estimate these parameters for heat balance analysis in and around the Japan Islands, we constructed a meteorological database and main processing system for thermal inertia mapping from aerometeorological and ground monitoring and NOAA satellite data, thus expanding the temperature estimation system (Fig. 1).

2. THERMAL INERTIA MODEL

Thermal inertia is the heat conductance capacity and has a specific value for each type of material. It determines heat diffusion in the soil or shallow part of the earth's crust. For construction of a TIMS, a thermal inertia model is the most important consideration, as expressed by:

$$|\lambda c| = \frac{dS}{dTs\sqrt{2\pi}}\sqrt{\tau_0} - \left(\sqrt{k}\,\rho Cp\,(1+\frac{l\,\mu\Phi}{Cp})\right)$$

...(Utsunomiya,1988,92) (1)

where λ: thermal conductivity of soil layer, c: specific heat of soil, r: specific gravity of soil, dTs and dS: daily range of surface temperature and net radiation, respectively, K: diffusion coefficient, τ°: periodic time, ρ: air density, Cp: specific heat of air at constant pressure, l: latent heat, μ: relative wetness of soil surface, Ø: gradient of the saturated vapor pressure curve

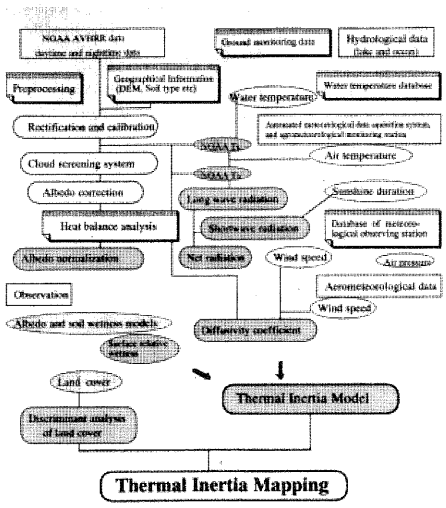

Fig. 1 Total system used for thermal inertia mapping.

3. CONSTRUCTION OF DATABASE AND PREPROCESSING

3.1 Construction of database

3.1.1 Prototype database for hydrological monitoring data: Water temperature is the basic elements of hydrological data. We obtained information on its attributes and sample data were collected by questionnaire from many monitoring stations in Japan. Also, the sample data were compiled and formatted by generation of these attributes from other databases such as the public use water quality datafile and Fisheries Information Center (Fig. 2).

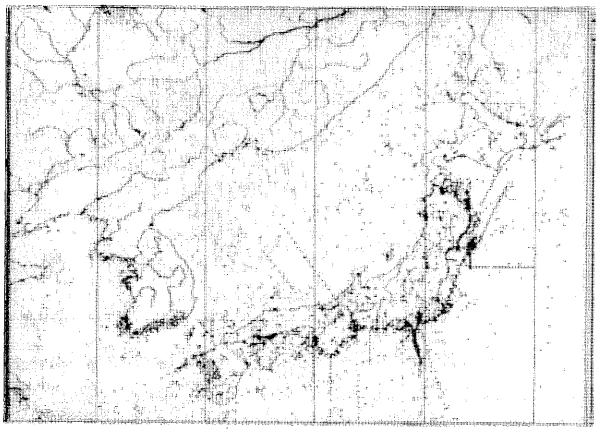

Fig. 2 Distribution of monitoring points of water temperature in and around the Japan Islands.

3.1.2 Prototype database for meteorological monitoring data in Japan: We obtained attributes from about 130 meteorological monitoring stations and their sample data using questionnaires. The meteorological prototype database was constructed in 1994. We were able to exclude noisy data for evaluating the circumstances of the monitoring station using height and distance from natural and artificial features, which affect the data (Fig. 3).

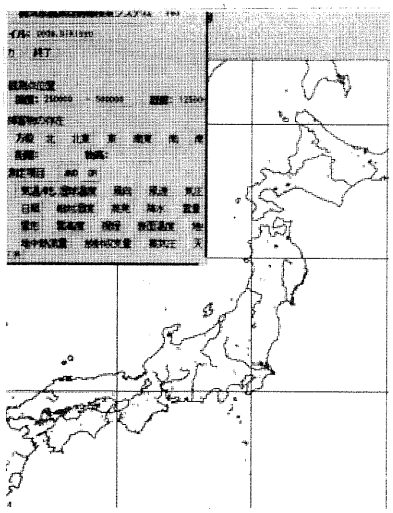

Fig. 3 Output of retrieval system of the meteorological database.

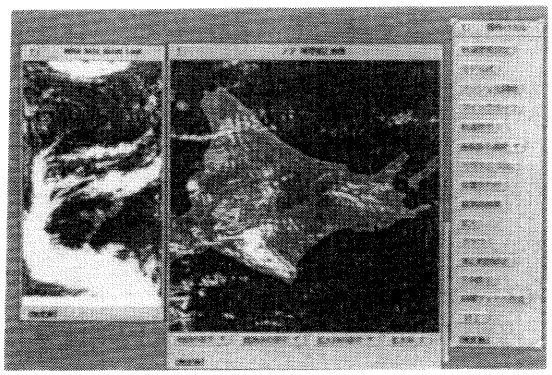

Fig. 4 Output of the results of rectification of NOAA imagery for Hokkaido, Japan.

3.2 Improvement of rectification system for NOAA AVHRR imagery.

A rectification system for NOAA imagery based on Sun's algorithm (Sun,1989) was elongated to allow efficient data retrieval from rectified NOAA image in TIMS (Fig. 4).

3.3 Cloud screening

Cloud screening is necessary to reduce the estimation error in statistical processing and to obtain the amplitudes of both the earth's surface temperature (Ts) and net radiation. A cloud screening subsystem was developed based on i) a color composite method (Utsunomiya *et al*, 1990; Bellec and Gleau, 1992), and ii) the PCA/ clustering procedure "PCTSMC" (Gallaudet and Simpson,1991) using brightness Ts derived from NOAA Channels 3, 4 and 5 (Fig. 5). These procedures were evaluated using NOAA daytime imagery of an area from Hokkaido to Sanriku (northeastern Honshu). The results of both procedures were similar, although the latter overeliminated the cloud-masked areas (Fig. 6).

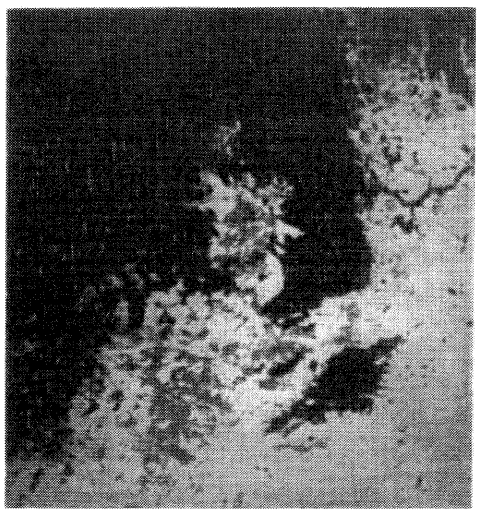

Fig. 5 Cloud screening based on the color composite method of NOAA imagery in northeastern China (after Utsunomiya et, al., 1990).

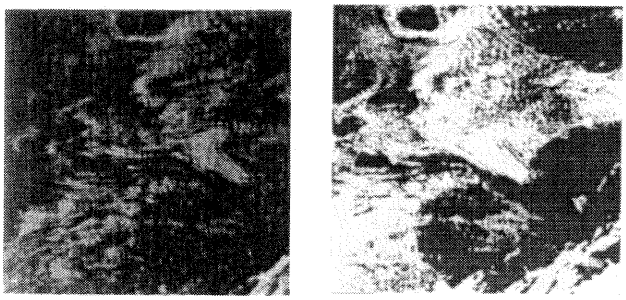

color composite PCTSMC

Fig. 6 Cloud screening based on color composite and PCTSMC methods of NOAA imagery in an area from Hokkaido to northeastern Honshu (after Utsunomiya and Katoh, 1995).

3.4 Surface and air temperatures

3.4.1 Determination of surface temperature: Surface temperature (Ts) in each NOAA pixel was calculated from the relationships between NOAA brightness temperature and water temperature retrieved from the above database.

3.4.2 Estimation of air temperature: Air temperature (Ta) in each NOAA pixel was also computed using a statistical model based on the relationships between surface temperature Ts and air temperature derived from the above database and other meteorological datafiles (Fig.7, 8).

3.4.3 Amplitude of temperature: The amplitudes of both surface and air temperature, dTs and dTa, in NOAA pixels were calculated by subtracting the temperatures Ts and Ta at night from each of those during the day, respectively.

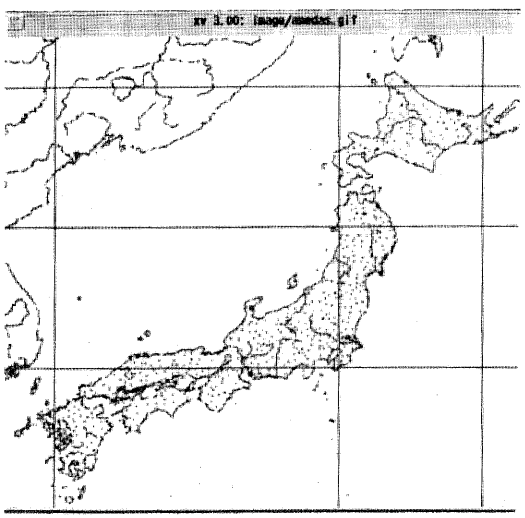

Fig. 7 Distribution of ground monitoring points in an automated meteorological data system for Japan.

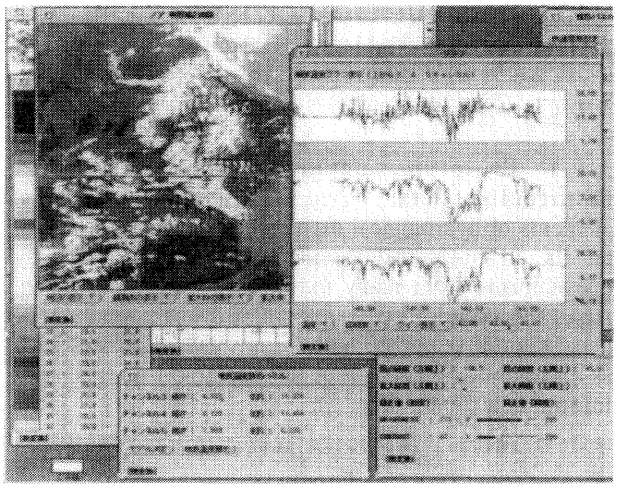

Fig. 8 Distribution of estimated air temperature, its profile, legend and operational panel.

4. HEAT BALANCE ANALYSIS

4.1 Shortwave radiation

4.1.1 Downward short-wave radiation: Downward short-wave radiation was calculated by the procedure suggested by Seino and Uchijima (1988) and statistical modeling was done from the relationships between TOVS and radiation data at the monitoring stations. Assuming the diurnal variation of solar radiation to be approximately sinusoidal on a cloudless day (Monteith, 1973), variation curves of direct and diffuse radiation were computed using following models. These parameters were computed in the following equation. First, solar radiation was calculated using parameters such as duration of sunshine, sun elevation and snow cover.

$$[StH] = S0 \left(0.146+0.534\frac{\tau}{\tau^{\circ}} + 0.047G10 + 0.036 \sin h'\right)$$

.....(Yoshida and Shinoki, 1978) (2)

where h: sun elevation at noon on the 15th day of each month, G10: index of snow cover; ratio of the number of days with snow cover exceeding 10 cm depth divided by the amount of days in any month, S0: monthly average duration of possible sunshine in any month
Monthly average of direct solar radiation [SbH] was calculated using following equation.

$$\frac{[SbH]}{[StH]} = -0.1528 + 0.9201\frac{[StH]}{S0} - 0.0013\, ea - 0.0706\, G10$$

.....(Seino and Uchijima, 1988) (3)

where [StH] : monthly average of global solar radiation

[SbH], [SdH] : monthly average daily amount of direct solar and diffuse radiations, respectively

$$ea = 4.54 \exp(0.068 \cdot Ta)$$ .....(Seino and Uchijima,1988) (4).

This equation for estimating vapor pressure, ea, was developed using data obtained in a humid climate. Ta: air temperature, G10: The index G10 is substituted by the index, G0, in the following equation, where G0 is the ratio of the number of days with any depth of snow

cover exceeding 0 cm divided by the number of days in any month

$$G_{10} = -0.277 + 0.014 \cdot Ta + 1.146 \cdot G_0 \quad \text{...(Seino and Uchijima, 1988) (5).}$$

The monthly average daily amount of diffuse radiation Sth was computed using the following equation;

$$[S_dH] = [S_tH] - [S_bH] \quad .....(6).$$

We calculated both of these diurnal variations in the hourly amount of direct solar and diffuse radiation by applying Seino and Uchijima models in the following:

$$S_bH(t)=[S_bH]\{A_0 + A_1\cos t + A_2\cos^2 t\}$$
...(Seino and Uchijima, 1988) (7)

$$S_dH(t)=[S_dH]\{B_0 + B_1\cos t + B_2\cos^2 t\}$$
.....(Seino and Uchijima, 1988) (7')

where $[S_bH]$, $[S_dH]$: monthly average daily amount of direct solar and diffuse radiation, respectively,

and t is deviation of the hour angle from that at southing. A and B are constants.

The simultaneous downward short-wave radiation coincident with NOAA daytime observation at each monitoring station was retrieved from the value indicated from restored energy variation curves. Then, the short-wave radiation at each station was interpolated to bring into registration with NOAA imagery(Fig. 9).

As for interpolation, the values on the four sides of a square map obligatorily have values such as minimum, average or zero. In this study, we assigned the values from the nearest monitoring points to any points on the sides. This procedure was applied to parameters such as the diffusion coefficient to conform with NOAA pixel data.

4.1.2 Parameters related to upward short-wave radiation: Albedo correction: Surface relative wetness is estimated from the absolute albedo derived from the correction of the percentage albedo multiplied by the sine of sun elevation, longitude and latitude parameters to first approximation. However, other components of heat balance analysis require the percentage albedo derived from the NOAA visible channel.

Normalization of albedo and surface relative wetness: The relative wetness of the soil surface is an indispensable parameter for the thermal inertia model. Wetness estimation models for both loamy and sandy soils were developed upon relationships between soil wetness within 1 cm depth and the absolute albedo of the soil surface derived from experimental data for upland fields on the terraces and the Kujukuri coastal plain, Central Japan (Fig.10). The relative wetness of the soil surface was calculated using the normalized absolute albedo μ' in each NOAA pixel in the following:

$$\mu' = 1 - \frac{\alpha' - \alpha\min}{\alpha\max - \alpha\min} \quad .....\text{(Utsunomiya, 1988,92) (8)}$$

where μ' : relative wetness of soil surface, α' : absolute albedo in each pixel of NOAA imagery, $\alpha\max$, $\alpha\min$: maximum and minimum absolute albedo derived from observed data.

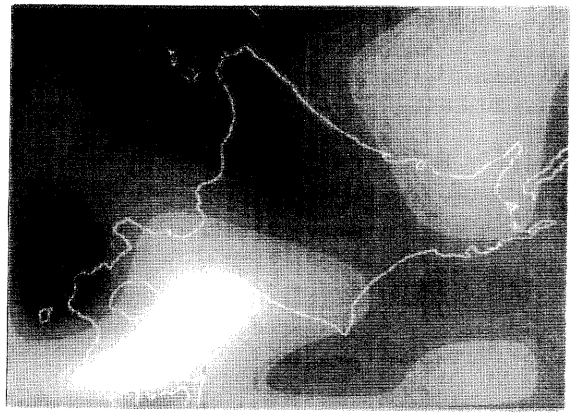

Fig. 9 Distribution of shortwave radiation in and around Hokkaido Island, Japan (Oct. 17,1990).

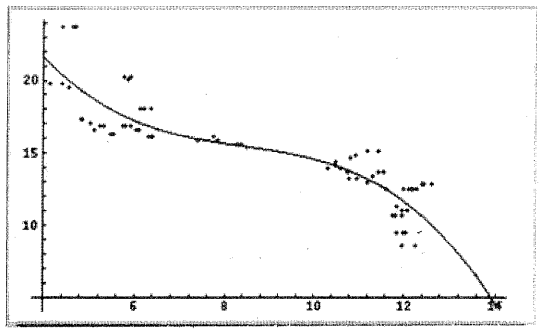

Fig. 10 Model for estimation of soil surface wetness (wetness of loamy soil from absolute albedo).

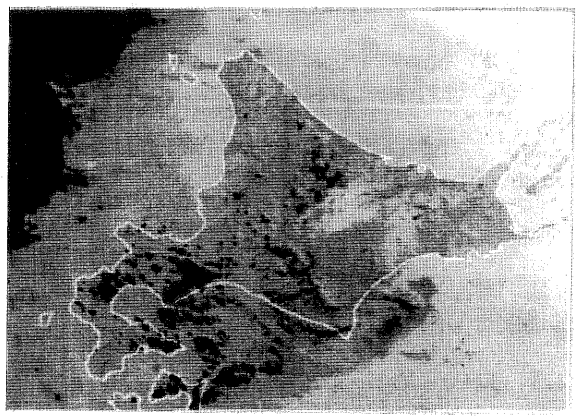

Fig. 11 Distribution of soil surface wetness (assuming that a model was applied to all pixels of NOAA imagery, Oct. 17,1990).

Figure 11 shows soil surface wetness in the Hokkaido Island, Japan. We assumed that a model was applied to all pixels of NOAA imagery.

4.2 Long wave radiation

Downward and upward long wave radiation was calculated from the empirical models.

4.2.1 Downward long wave radiation: Downward long wave radiation (D) was calculated from the following empirical model.

$$L = \sigma T^4 \{0.61 - 0.058 \sqrt{e}\} \quad .....(9)$$

where T: temperature (K°), e: vapor pressure (mmHg). Vapor pressure e is computed using the equation:

$$e = ew(t') - Cp\, P / 0.6221 (t - t') \quad .....(10)$$

where e: vapor pressure (mb), Cp: specific heat of air at constant pressure, P: air pressure, l: 580 cal/g, t,' t: temperature of wet and dry thermocouple thermometers, ew: saturated vapor pressure.
In remote sensing, difficulties with the measurement of wet-bulb temperature make it necessary to assume that both wet and dry bulb thermometers' temperatures are equal. Therefore, we applied the above Seino and Uchijima vapor pressure model based on data for a humid climate. Similar vapor pressure models are expected to develop for application in regions with different climates.
Figure 12 shows daytime downward long wave radiation in the Hokkaido Island, Japan.

4.2.2 Upward long wave radiation: Upward long wave radiation is estimated by the following equation:

$$U = \delta\sigma(Ts + 273.15)^4 + (1 - \delta) L \quad .....(11)$$

where δ: emissivity, σ: Stefan Boltzmann constant, Ts: surface temperature (C°), L: downward long wave radiation
Figure 13 shows daytime upward long wave radiation in the Hokkaido Island, Japan.

4.2.3 Effective radiation: Then, effective radiation (F) is calculated using the following equation:

$$F = L - U \quad .....(12)$$

where F: effective radiation, L: downward longwave radiation, U: upward longwave radiation.

4.3 Net radiation

Net radiation (S) is obtained by the following;

$$S = (1 - \alpha')R - F \quad .....(13)$$

where S: net radiation, a': albedo (estimated albedo in each pixel), R: downward short-wave radiation, F: effective radiation.
Each net radiation during the day and at night was calculated by this process, and the amplitude of net radiation dS was obtained by subtracting net radiation at night from that during the day.
Figure 14 shows daytime net radiation in the Hokkaido Island, Japan.

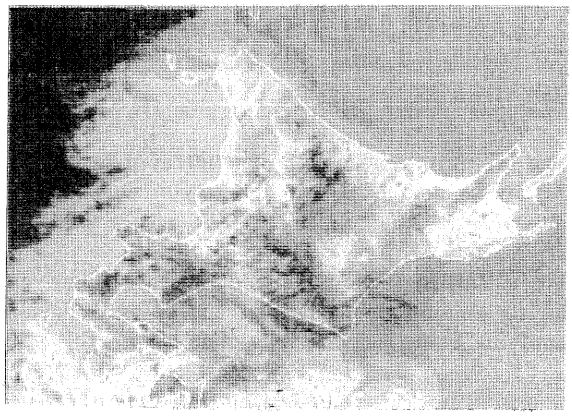

Fig. 12 Distribution of downward longwave radiation in and around Hokkaido Island, Japan (Oct. 17, 1990).

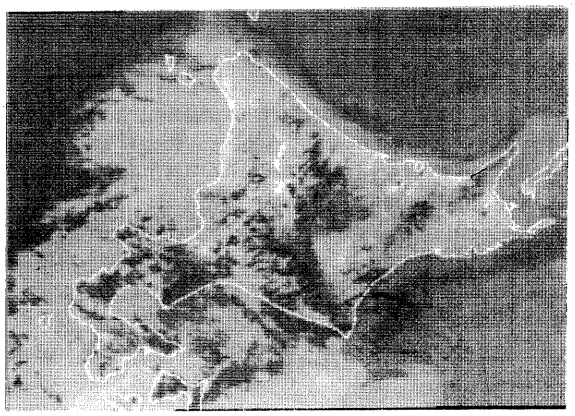

Fig. 13 Distribution of upward longwave radiation in and around Hokkaido Island, Japan (Oct. 17, 1990).

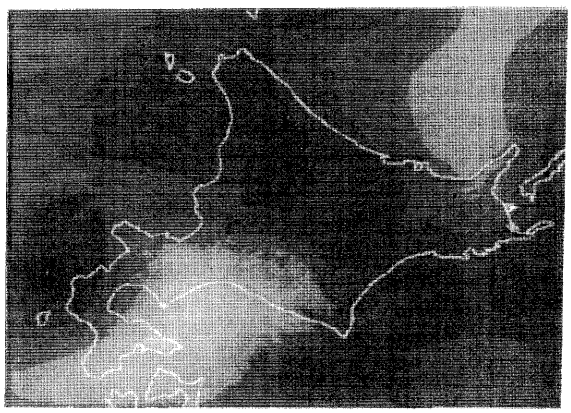

Fig. 14 Distribution of net radiation in and around Hokkaido Island, Japan (Oct. 17,1990).

4.4 Diffusion coefficient

The diffusion coefficient was obtained using both approaches based on surface roughness using formulae for the logarithmic law of wind velocity and heat transfer. The former was suggested by Kondo and Yamasawa (1983).

4.4.1 Roughness estimation: Surface roughness is calculated using relationships between wind velocity at an isobaric surface of 800 - 900 mb and that at the ground meteorological monitoring station in the procedure suggested by Kondo and Yamasawa (1983).
First, the geostropheric wind speed is calculated using the following equation

$$G = V_{900} - \frac{V_{800} - V_{900}}{2} \quad \text{..... (14)}$$

where G, V_{800}, and V_{900} is geostrophic wind speed and wind speed at isobaric surfaces of 800 and 900 mb, respectively.

Then, the G values from wind data at aerometeorological stations were interpolated to make it correspond with the points of the ground meteorological monitoring stations (Automated Meteorological Data Aquisition System).
U*/G can be converted to Vz/G in the following deformed formula for the logarithmic law of wind velocity;

$$\frac{Vz}{G} = \frac{U^*}{G} \cdot \frac{1}{\kappa} \cdot \ln\left(\frac{Z}{Z_0}\right) \quad \text{.....(15)}$$

where Vz: Daily average of wind speed at a ground meteorological station, G: geostrophic wind speed at an isobaric surface of 800 - 900 mb, U*: surface friction velocity, k: Karman's constant, Z0: roughness, Z: altitude of wind gauge (Z=Z-d). Here, in this study, zero-plane displacement (d) is also assumed as zero in the same way as for Kondo and Yamazawa (1983).
Surface roughness is given in the following equation;

$$\ln\frac{G}{f Z_0} = A - \ln Cg + \left(\frac{k^2}{Cg^2} - B^2\right)^{\frac{1}{2}}$$

..... (Kondo and Yamasawa, 1983) (16)

where G: geostrophic wind speed at an isobaric surface of 800 - 900 mb, Cg: U*/ G, f: 2 ω sin ϕ (Coriolis factor), f: latitude, A: 1.5, B: 4, U*: surface friction velocity, k: Karman's constant, Z0: roughness.

4.4.2 Estimation of diffusion coefficient: Substitution of roughness (Z0) into equation (Eq.15) gives the surface friction velocity (U*).
Then, we can obtain the diffusion coefficient (K) by substituting the surface friction velocity (U*) into the following equation:

$$K = U^* \cdot k \cdot Z \quad \text{.....(17)}$$

where K: diffusion coefficient, U*: surface friction velocity, k: Karman's constant, Z: altitude of wind gauge.

Then the diffusion coefficients obtained from the meteorological monitoring stations were interpolated to coincide to each NOAA image pixel in the same way as for shortwave radiation. The value on both sides of the mapping frame was obligatorily given by the values of the diffusion coefficient at the nearest monitoring points (Fig.15).

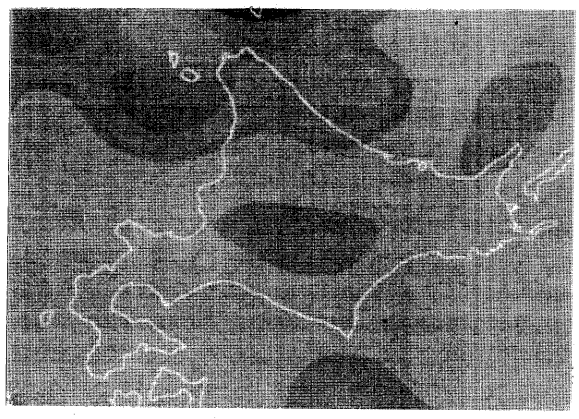

Fig. 15 Distribution of diffusion coefficient in and around Hokkaido Island, Japan (Oct. 17,1990).

4.5 Determination of gradient of the saturated vapor pressure curve

For the last parameter of the thermal inertia model, it is necessary to determine the inclination of the saturated vapor pressure model/curve based on the relationships between temperature and saturated vapor pressure. The gradient of the tangent to the curve was obtained as a differential coefficient at an average value of air and surface temperatures.

5. THERMAL INERTIA

Parameters such as downward/ upward shortwave and long wave radiation, daily amplitude of both surface and air temperatures and net radiation, relative wetness of soil surface and diffusion coefficient were derived from the above heat balance analyses using meteorological and NOAA AVHRR data obtained at noon and in the early morning (here, nighttime data were used instead of those for early morning). It is then, possible to compute the thermal inertia in each NOAA AVHRR image pixel by substituting these parameters into the thermal inertia model (Eq.1).

6. CONCLUSIONS

In this study, the author constructed a prototype database of attributes and sample data from ground meteorological and hydrological monitoring stations. By feeding the other data such as information from aerometeorological and ground meteorological stations into this database, and integrating it with geographical

information, a main processing system for heat balance analysis in our thermal inertia mapping system (TIMS) was developed for heat balance and hydrological evaluation in northeast Asia. This system using NOAA satellite data was expanded from my approach discussed earlier using air and spaceborne MSS data. Although some parameters or models in our module still need to be improved, this construction of a TIMS for satellite remote sensing data is almost complete, substituting physical quantities such as the diffusion coefficient and downward shortwave radiation into our analytically developed thermal inertia model.

7. ACKNOWLEDGMENT

The author wishes to thank Dr. Zenbei Uchijima, Professor of Miyazaki Municipal University, who offered advice during this study, and Dr. Hiroshi Seino, National Institute of Agro-environmental Sciences, who helped in the construction of our system for installation of his program.

8. REFERENCES

Ångstrom, A. (1925): The albedo of various surfaces of ground. Geografiska Analar, 7, 323-342.

Bellec, B. and H. Le Gleau (1992): The multispectral colour-composite technique: an improved method to display meteorological satellite imagery. Int. J. Remote Sensing, 13,11, 1981-1998.

Gallaudet, T. C., and J. Simpson (1991): Automated cloud screenings of AVHRR imagery using split and merge clustering. Remote Sensing Environment, 38, 77-121.

Kondo, J. and H. Yamazawa (1983): Surface wind speed and aerodynamic roughness over complex ground surface. Tenki, 30, 553-561. (J)

Monteith, J. L. (1980): Principles of Environmental Physics. Edward Arnold, London, p.241.

Nakagawa, S. (1982): Seasonal and diurnal variations of albedo for a field of pasture. Hydrology, 12, 7-11. (J)

NOAA (1986): NOAA polar orbitor data [TIROS-N, NOAA-6, NOAA-7, NOAA-8, NOAA-9,and NOAA-10] Usr Guide [103 leaves]

NOAA (1988): Appendix B to NOAA TM for NOAA-H/11. Sept. 20, 1988 [23 leaves]

NOAA (1986): Data extraction and calibration of TIROS-N/NOAA radiometers. NOAA- Technical Memorandom NESS 107, Rev. 1, 58p. Appendix [42 leaves]

Seino, H. and Z. Uchijima (1988): An evaluation method of solar radiation resources on complicated terrain using topographical mesh data. 2-29. Estimation of natural energy resources. Tokyo, Agriculture, Forestry and Fishery Research Council Secretariat (J,E)

Sun, W. D. (1989): A geometric distortion correction method and atmospheric correction for NOAA satellite imageries. 165P. A Doctoral Dissertation presented to University of Tokyo. (J)

Utsunomiya, Y. (1988): Soil moisture estimation based on thermal inertia from airborne MSS measurements. Int. Archives of Photogrammetry and Remote Sensing, V27, B7, IV, 663-672.

Utsunomiya, Y., Zhao, H., Hua, R., and B. Yu (1990): Soil moisture mapping based on thermal inertia from NOAA-11 satellite AVHRR measurements. J. Geography, 99, 483-489. (J,E)

Utsunomiya, Y. (1992): Theoretical analysis of a thermal inertia model for soil moisture estimation and its application to remote sensing. J. Japan Society of Photogrammetry and Remote Sensing, 31(4) 15-26.

Utsunomiya, Y. (1992): Construction of a global environment database from satellite remote sensing data - estimation of air temperature on Kyushu Island, southern Japan, from Landsat data and ground station meteorological data. Int. Archives ISPRS, 29, B4, IV, 406-411.

Utsunomiya, Y., Tsunekawa, A. and S. Katoh (1993): Construction of a database for heat balance analysis based on earth observation data and its interpretations (2): Questionnaire of water temperature monitoring station, its datafile and retrieval system, and mapping. Proceedings of Autumn meeting of Japanese Geographical Society, 44, 210-211. (J)

Utsunomiya, Y., Tsunekawa, A. and S. Katoh (1993): Construction of a database for heat balance analysis based on earth observation data and its interpretations (3): Estimation of air temperature, and its mapping. Proceedings of 15th Meeting of Remote Sensing Society of Japan, 185-186. (J)

Utsunomiya, Y., Tsunekawa, A. and S. Katoh (1994): Construction of a database for heat balance analysis based on earth observation data and its interpretations (4): Geographical information, temperature, its retrieval and mapping. Proceedings of Spring meeting of Japanese Geographical Society, 45, 342-343. (J)

Utsunomiya Y., and T. Yamaguchi (1995): Soil moisture estimation based on thermal inertia from airborne MSS measurements in the Kujukuri coastal plain, Central Japan. J. Remote Sensing Society of Japan, 15, 242-253. (J,E)

Utsunomiya Y. (1995): Construction of a database for heat balance analysis based on earth observation data and its interpretations (7): An automatic cloud screening of NOAA AVHRR data. Proceedings of Autumn Meeting of Japan Geographical Society, 48, 188-189. (J)

Utsunomiya Y., and S. Katoh (1995): Construction of a database for heat balance analysis based on earth observation data and its interpretations (8) - an automatic cloud screening of NOAA AVHRR data (part 2). Proceedings of 21st Remote Sensing Symposium, 99-102. (J)

Utsunomiya, Y., Fujinuma, Y., and J. Katoh (1996): Shortwave radiation: An important parameter of thermal inertia mapping system (TIMS). Proceeding of 6th Global Environmental Monitoring from Space (GEMS) Forum, 125-129. (J,E)

Yoshida, S. and S. Shinoki (1978): Preparation of maps of monthly mean global solar radiation and its year to year variability for the Japanese Islands. Tenki, 25, 375-389. (J)

Yoshida, S. and S. Shinoki (1983): Maps of monthly mean sky and direct solar radiation on the horizontal surface for Japan. Tenki, 30, 201-216. (J)

(J: Japanese, J,E: Japanese with English abstract)